Eur. Phys. J. Special Topics **229**, 2429–2441 (2020) © EDP Sciences, Springer-Verlag GmbH Germany, part of Springer Nature, 2020 https://doi.org/10.1140/epjst/e2020-000178-3

THE EUROPEAN
PHYSICAL JOURNAL
SPECIAL TOPICS

Regular Article

# Emergent symplectic symmetry in atomic nuclei

### Ab initio symmetry-adapted no-core shell model

Kristina D. Launey<sup>1,a</sup>, Tomáš Dytrych<sup>1,2</sup>, Grigor H. Sargsyan<sup>1</sup>, Robert B. Baker<sup>3</sup>, and Jerry P. Draayer<sup>1</sup>

Received 29 July 2020 / Accepted 28 August 2020 Published online 23 October 2020

**Abstract.** Exact symmetry and symmetry-breaking phenomena play a key role in gaining a better understanding of the physics of manyparticle systems, from quarks and atomic nuclei, through molecules and galaxies. In nuclei, exact and dominant symmetries such as rotational invariance, parity, and charge independence have been clearly established. Beyond such symmetries, the nature of nuclear dynamics appears to exhibit a high degree of complexity, and only now, we show the fundamental role of an emergent approximate symmetry in nuclei, the symplectic  $Sp(3,\mathbb{R})$  symmetry, as clearly unveiled from ab initio studies that start from realistic interactions. In this article, we detail and enhance our recent findings presented in [T. Dytrych, K.D. Launey, J.P. Draayer, D.J. Rowe, J.L. Wood, G. Rosensteel, C. Bahri, D. Langr, R.B. Baker, Phys. Rev. Lett. 124, 042501 (2020), that establish  $Sp(3,\mathbb{R})$  as a remarkably good symmetry of the strong interaction, and point to the predominance of a few equilibrium nuclear shapes (deformed or not) with associated vibrations and rotations that preserve the symplectic  $Sp(3,\mathbb{R})$  symmetry. Specifically, we find that the structure of nuclei below the calcium region in their ground state, as well as in their low-lying excited states and giant resonances, respects this symmetry at the 60–80% level.

### 1 Introduction

We have recently shown through first-principle large-scale nuclear structure calculations that the special nature of the strong nuclear force determines highly regular patterns in nuclei that can be tied to an emergent approximate symmetry [1]. We find that this symmetry is remarkably ubiquitous, regardless of the type of the nucleus

Department of Physics and Astronomy, Louisiana State University, Baton Rouge, LA 70803, USA

 $<sup>^2</sup>$  Nuclear Physics Institute, Academy of Sciences of the Czech Republic, 250 68 Řež, Czech Republic

<sup>&</sup>lt;sup>3</sup> Institute of Nuclear and Particle Physics, and Department of Physics and Astronomy, Ohio University, Athens, OH 45701, USA

a e-mail: klauney@lsu.edu

and the particular strong interaction heritage, and mathematically tracks with a symplectic group. For a set of A particles, the symplectic symmetry  $\operatorname{Sp}(3,\mathbb{R})$  is based on a very basic concept: linear canonical transformations of particle coordinates and momenta that preserve the fundamental Heisenberg commutation relation, as detailed in Section 2. The most interesting insight, however, arises from a complementary perspective: the symplectic symmetry has been recognized to preserve an equilibrium shape under transformations, such as rotations, orientations in space, and vibrations [2]. This, in turn, has important implications to our understanding of the physics of nuclei: the approximate symplectic symmetry is manifested in nuclear states as the predominance of only a few symplectic irreducible representations (or irreps, subspaces of configurations that preserve the symmetry). Hence, we now understand that nuclei are made of only a few equilibrium shapes, deformed or not, with associated vibrations and rotations.

In this paper, we detail that dominant features of light to intermediate-mass nuclei (below the calcium region), including their low-lying excited states and giant resonances, track with the symplectic symmetry and naturally emerge from first-principle (ab initio) considerations, even in close-to-spherical nuclear states without any recognizable rotational properties. Therefore, the present outcomes not only explain but also predict the emergence of nuclear collectivity.

To study this without limitations within the interaction and approximations during the many-body nuclear simulations, we use the *ab initio* symmetry-adapted no-core shell model (SA-NCSM) [1,3,4]. The model starts with realistic interactions tied to elementary particle physics considerations and fitted to nucleon-nucleon scattering data, and uses symmetry-adapted (SA) bases based on the Sp(3,  $\mathbb{R}$ ) symmetry and its subgroup, the deformation-related SU(3). The Sp(3, $\mathbb{R}$ ) approximate symmetry is utilized to dramatically reduce computational resources required in *ab initio* large-scale modeling of nuclear structure and reactions. This, in turn, pioneers predictions in open-shell deformed intermediate-mass nuclei, such as Ne and Mg isotopes [1,5–7], and targets short-lived isotopes with enhanced deformation or cluster substructure along various nucleosynthesis pathways, especially where experimental measurements are incomplete or not available.

## 2 Symplectic and SU(3) symmetries

It is well known that SU(3) [8–12] is the symmetry group of the spherical harmonic oscillator (HO) that underpins the shell model [13] and the valence-shell SU(3) (Elliott) model [8,14,15] (for technical details of SU(3), see reference [16]). The Elliott model has been shown to naturally describe rotations of a deformed nucleus without the need for breaking rotational symmetry. The key role of deformation in nuclei and the coexistence of low-lying quantum states in a single nucleus characterized by configurations with different quadrupole moments [17] makes the quadrupole moment adominant fundamental property of the nucleus. Hence, the quadrupole moment and the monopole moment or "size" of the nucleus, along with nuclear masses, establishes the energy scale of the nuclear problem. Indeed, the nuclear monopole and quadrupole moments underpin the essence of symplectic  $Sp(3,\mathbb{R})$  symmetry.

The symplectic group  $\operatorname{Sp}(3,\mathbb{R})$  consists of all particle-independent linear canonical transformations of the single-particle phase-space observables, the positions  $\mathbf{r}_i$  and momenta  $\mathbf{p}_i$  (with particle index  $i=1,\ldots,A$  and special directions  $\alpha,\beta=x,y,z$ )

$$r'_{i\alpha} = \sum_{\beta} A_{\alpha\beta} r_{i\beta} + B_{\alpha\beta} p_{i\beta} \tag{1}$$

$$p'_{i\alpha} = \sum_{\beta} C_{\alpha\beta} r_{i\beta} + D_{\alpha\beta} p_{i\beta} \tag{2}$$

that preserve the Heisenberg commutation relations  $[r_{i\alpha}, p_{j\beta}] = i\hbar \delta_{ij} \delta_{\alpha\beta}$  [2,4,18]. Generators of these transformations, symbolically denoted as matrices  $\bf A$ ,  $\bf B$ ,  $\bf C$ , and  $\bf D$ , are constructed as "quadratic coordinates" in phase space,  $\bf r_i$  and  $\bf p_i$ , and, most importantly, sum over all the particles and act on the space orientation [on the contrary, the generators of the complementary O(A) sum over the three spatial directions and act on the particle index, with a growing complexity with increasing particle number]. Hence, the generators include physically relevant operators: the total kinetic energy  $(\frac{p^2}{2} = \frac{1}{2} \sum_i {\bf p}_i \cdot {\bf p}_i)$ , the monopole moment  $(r^2 = \sum_i {\bf r}_i \cdot {\bf r}_i)$ , the quadrupole moment  $(Q_{2M} = \sqrt{16\pi/5} \sum_i r_i^2 Y_{2M}(\hat{r}_i))$ , the orbital momentum  $({\bf L} = \sum_i {\bf r}_i \times {\bf p}_i)$ , and the many-body harmonic oscillator Hamiltonian  $(H_0 = \frac{p^2}{2} + \frac{r^2}{2})$ .

Another key feature is that a single-particle Sp(3,  $\mathbb{R}$ ) irrep spans all positive-parity

Another key feature is that a single-particle  $\operatorname{Sp}(3,\mathbb{R})$  irrep spans all positive-parity (or negative-parity) states for a particle in a three-dimensional spherical or triaxial (deformed) harmonic oscillator. Not surprisingly, the symplectic  $\operatorname{Sp}(3,\mathbb{R})$  symmetry, the underlying symmetry of the symplectic rotor model [18,19], has been found to play a key role across the nuclear chart – from the lightest systems [20,21], through intermediate-mass nuclei [4,22,23], up to strongly deformed nuclei of the rare-earth and actinide regions [18,24–26]. The results agree with experimental evidence that supports formation of enhanced deformation and clusters in nuclei, as well as vibrational and rotational patterns, as suggested by energy spectra, electric monopole and quadrupole transitions, radii and quadrupole moments [5,17,27]. And while these earlier algebraic models have been very successful in explaining dominant nuclear patterns, they have assumed symmetry-based approximations and have often neglected symmetry mixing. This establishes  $\operatorname{Sp}(3,\mathbb{R})$  as an effective symmetry for nuclei, which may or may not be badly broken in realistic calculations. It is then imperative to probe if this symmetry naturally arises within an *ab initio* framework, which will, in turn, establish its fundamental role.

## 3 Many-body symmetry-adapted (SA) framework

Ab initio approaches (e.g., see Ref. [28] and references therein) build upon a "first principles" foundation, namely, the properties of only two or three nucleons that are often tied to symmetries and symmetry-breaking patterns of the underlying quantum chromodynamics theory. We utilize the *ab initio* nuclear shell-model theory [29–31] that solves the many-body Schrödinger equation for A particles,

$$H\Psi(\mathbf{r}_1, \mathbf{r}_2, \dots, \mathbf{r}_A) = E\Psi(\mathbf{r}_1, \mathbf{r}_2, \dots, \mathbf{r}_A). \tag{3}$$

In its most general form, it is an exact many-body "configuration interaction" method, for which the interaction and basis configurations are as follows.

The intrinsic non-relativistic nuclear Hamiltonian  $H = T_{\rm rel} + V_{NN} + V_{3N} + \ldots + V_{\rm Coulomb}$  includes the relative kinetic energy  $T_{\rm rel} = \frac{1}{A} \sum_{i < j}^{A} \frac{(\mathbf{p}_i - \mathbf{p}_j)^2}{2m}$  (m is the nucleon mass), the nucleon-nucleon  $V_{NN}$  and, possibly, three-nucleon  $V_{3N}$  interactions and

 $<sup>^{1}</sup>$  A familiar example for an effective symmetry is SU(3). While the Elliott model with a single SU(3) irrep explains ground-state rotational states in deformed nuclei, the SU(3) symmetry is, in general, largely mixed, mainly due to the spin-orbit interaction (nonetheless, SU(3) has been shown to be an excellent quasi-dynamical symmetry, that is, each rotational state has almost the same SU(3) content [26]).

beyond, typically derived in the chiral effective field theory [32–35], along with the Coulomb interaction between the protons.

The method adopts a complete orthonormal many-particle basis  $\psi_k$ , such as the antisymmetrized products of single-particle states of a spherical harmonic oscillator of characteristic length  $b = \sqrt{\frac{\hbar}{m\Omega}}$ . The expansion  $\Psi(\mathbf{r}_1, \mathbf{r}_2, \dots, \mathbf{r}_A) = \sum_k c_k \psi_k(\mathbf{r}_1, \mathbf{r}_2, \dots, \mathbf{r}_A)$  renders equation (3) into a matrix eigenvalue equation with unknowns  $c_k$ ,  $\sum_{k'} H_{kk'} c_{k'} = E c_k$ , where the many-particle Hamiltonian matrix elements  $H_{kk'} = \langle \psi_k | H | \psi_{k'} \rangle$  are calculated for the given interaction and the solution  $\{c_k^2\}$  defines a set of probability amplitudes.

However, in *ab initio* shell-model calculations the complexity of the nuclear problem dramatically increases with the number of particles, and when expressed in terms of literally billions of shell-model basis states, the structure of a nuclear state is unrecognizable. But expressing it in a more informative basis, the symmetry-adapted (SA) collective basis [3,4], leads to a major breakthrough: we observe the incredible simplicity of nuclear low-lying states and the dominance of an approximate symmetry of nuclear dynamics, the symplectic  $\operatorname{Sp}(3,\mathbb{R})$  symmetry, which together with its slight symmetry breaking naturally describe atomic nuclei.

The SA-NCSM is reviewed in reference [4] and has been first applied to nuclei below the calcium region using the SU(3)-adapted basis [36] and the  $Sp(3,\mathbb{R})$ adapted basis [1]. Briefly, the many-nucleon basis states of the SA-NCSM are constructed using efficient group-theoretical algorithms [37] and are labeled according to  $SU(3)_{(\lambda \mu)} \times SU(2)_S$  by the total intrinsic spin S and  $(\lambda \mu)$  quantum numbers with  $\lambda = N_z - N_x$  and  $\mu = N_x - N_y$ , where  $N_x + N_y + N_z = N \le N_{\text{max}}$  for a total of N HO quanta distributed in the x, y, and z direction. Hence, e.g.,  $N_x = N_y = N_z$ , or equally  $(\lambda \mu) = (00)$ , describes a spherical configuration, while  $N_z$  larger than  $N_x = N_y$ , or  $\mu = 0$ , indicates prolate deformation. Hence, the model space is reorganized to subspaces that have fixed deformation, specified by U(3) and its quantum numbers  $N(\lambda \mu)$ . One can further organize these deformed configurations to subspaces that are associated with a fixed shape (here referred to as "equilibrium shape" or simply "shape"), labeled by a single deformation  $N_0(\lambda_0 \mu_0)$ . These subspaces, specified by  $Sp(3,\mathbb{R})$ , include the equilibrium shape, its vibrations (referred to as "dynamical shapes") and rotations. For example, a symplectic irrep 0(80) consists of a prolate equilibrium shape with  $\lambda_0 = 8$  and  $\mu_0 = 0$  in the 0p-0h (0-particle-0-hole) subspace (valence shell), along with many other deformed configurations, or dynamical shapes, that include particle-hole excitations to higher shells.

As for the inter-nucleon interaction, it is unitarily transformed to the SA basis, with matrix elements reduced with respect to  $SU(3) \times SU(2)$  (outlined in Refs. [38] and [39]). We note that while the model utilizes symmetry groups to construct the basis, calculations are not limited a priori by any symmetry and employ a large set of basis states that can, if the nuclear Hamiltonian demands, describe a significant symmetry breaking.

In references [36,40,41], we have shown that the SA-NCSM can use a significantly reduced number of SU(3)-adapted basis states (selected model spaces) as compared to the corresponding large complete  $N_{\rm max}$  model space without compromising the accuracy for various observables, including energies, point-particle proton and matter rms radii, electric quadrupole and magnetic dipole moments, reduced electromagnetic B(E2) transition strengths, and electron scattering form factors. In addition, we have shown that, for these selected spaces, the size of the model space and the number of nonzero Hamiltonian matrix elements grow slowly with  $N_{\rm max}$  [40], allowing the SA-NCSM to accommodate model spaces of larger  $N_{\rm max}$  and to reach heavier nuclei, with recent SA-NCSM results reported for  $^{32}$ Ne and  $^{48}$ Ti [42].

To achieve this, in the SA-NCSM all basis states are kept up to a given N, while for higher N, the model space is down selected in a systematic way using  $\operatorname{Sp}(3,\mathbb{R})$ 

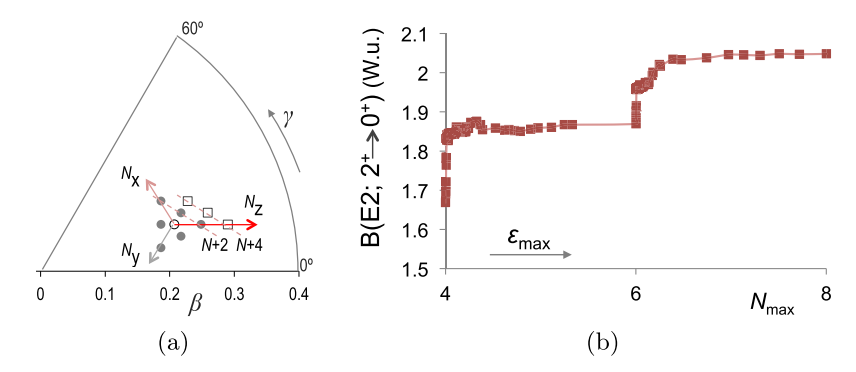


Fig. 1. (a) Selection of configurations in N+4 (open squares) based on dominant N+2 configurations, shown in terms of the deformation  $\beta$  and triaxiality  $\gamma$  shape parameters [43,44]. N+2 configurations (filled circles) within a symplectic irrep are determined by the kinetic energy or quadrupole operator (for monopole or quadrupole symplectic excitations, respectively), or equivalently, by the number of all possible ways two HO quanta are distributed in the x, y, and z directions. (b) Convergence of the B(E2;  $2_1^+ \to 0_{\rm gs}^+$ ) strength in  $^{12}{\rm C}$  with the SA-NCSM selection cutoff,  $\varepsilon_{\rm max}$ , for the JISP16 NN interaction [45] and  $\hbar\Omega=20~{\rm MeV}$ .

considerations (Fig. 1a). Configurations that are highly favored in the N model space inform important configurations in the N+2 model space, which in turn inform the N+4 model space, etc., and those track with larger deformation  $\beta$  along the  $N_z$  axis (consistent with results in Refs. [23,46]). Notably, these N+4 configurations can be readily reached from the N+2 configurations in the  $N_z$ - $N_x$  plane by two excitations in the z direction. Hence, we can introduce a selection cutoff  $\varepsilon_{\text{max}}$ , that is given by the fraction of the SA model space used. The order in which basis states are included is determined according to a weight  $w(N_x, N_y, N_z + 2) = \frac{P(N_x, N_y, N_z)}{\dim(N_x, N_y, N_z + 2)}$ , where  $P(N_x, N_y, N_z)$  is the probability amplitude obtained in SA-NCSM calculations in the N model space, and dim denotes the dimensionality of the configuration to be selected (spin degrees are omitted for simplicity). The prescription is then applied to N+4up through  $N_{\text{max}}$ . Similar to NCSM, a measure of convergence of the results is the degree to which the SA-NCSM obtains results independent of the model parameters  $N_{\rm max}$ ,  $\hbar\Omega$ , and  $\varepsilon_{\rm max}$  [see Fig. 1b for increasing  $\varepsilon_{\rm max}$ ]. Remarkably, even for small  $\varepsilon_{\rm max}$  cutoffs, which correspond to drastically reduced model spaces, observables such as, e.g., B(E2) values are quite close to the converged results, a feature that further improves with  $N_{\text{max}}$ . A major advantage of the SA-NCSM is that the SA model space can be down-selected to a subset of SA basis states that describe equilibrium and dynamical shapes, and within this selected model space the spurious center-of-mass motion can be factored out exactly [47,48].

In SA-NCSM calculations that use the Sp(3,  $\mathbb{R}$ )-adapted basis [1], the basis is built from the SU(3)-adapted basis. The difficulty stems from the fact that there are no known Sp(3,  $\mathbb{R}$ ) coupling/recoupling coefficients, and one has to resort to innovative techniques. In our method, we adopt the SU(3) scalar operator  $\{A^{(2\,0)} \times B^{(0\,2)}\}_{L=0M=0}^{(0\,0)}$  constructed by symplectic Sp(3,  $\mathbb{R}$ ) generators, where  $B_{LM}^{(0\,2)} = (-)^{L-M} (A_{L-M}^{(2\,0)})^{\dagger}$  is conjugate to  $A^{(2\,0)}$  and moves a particle two shells down. This SU(3) scalar operator is computed for a given set of basis states with the same  $N(\lambda \mu)$ ; eigenvectors of this matrix realize Sp(3,  $\mathbb{R}$ )-adapted basis states and provide a unitary transformation from the SU(3)-adapted basis to the Sp(3,  $\mathbb{R}$ )-adapted basis, while the known eigenvalues are used to assign each eigenvector to a specific

symplectic irrep. Given the unitary transformation, the SU(3)-decomposed Hamiltonian is straightforwardly constructed for the new  $Sp(3,\mathbb{R})$  basis. In selected model spaces, the resulting Hamiltonian matrix is then drastically small in size and its eigensolutions, the nuclear energies and states, can be calculated without the need for supercomputers.

# 4 Nature's preference: approximate symplectic symmetry from first principles

We report on the remarkable outcome, as unveiled from first-principle calculations below the calcium region, that nuclei exhibit relatively simple physics. We now understand that a low-lying nuclear state is predominantly composed of a few equilibrium shapes that vibrate and rotate, with each shape characterized by a single symplectic irrep. For example, in  $^{20}$ Ne, there is a single most predominant irrep, (80), that make up about 70% or more of the ground state (Fig. 2a) and its rotational excitations [1]. Using this single Sp(3,  $\mathbb{R}$ ) irrep, it is notable that even excitation energies and B(E2) strengths fall closely to the experimental data (Fig. 2b). Indeed, E2 transitions are determined by the quadrupole operator Q, an Sp(3,  $\mathbb{R}$ ) generator that does not mix symplectic irreps – hence, the largest fraction of these transitions, and hence nuclear collectivity, necessarily emerges within this most dominant symplectic irrep (similarly for rms radii, since  $r^2$  is also a symplectic generator).

To report observables, we use extrapolations to the infinite number of shells (independent of model parameters  $N_{\rm max}$  and  $\hbar\Omega$ ). They are based on the fast convergence we observe for nuclear properties, such as energies and B(E2) strengths, within a set of symplectic irreps and around an optimum  $\hbar\Omega$  value (Figs. 2c and 2d). Hence, for data on a converging trend, one can use the Shanks transformation ansatz for a quantity  $X_{\infty} = \sum_{n=0}^{\infty} x_n$  such that  $X_N = \sum_{n=0}^N x_n$  is given by  $X_N = X_{\infty} + Aq^N$  for large N, where 0 < q < 1 [50,51].  $X_{\infty}$  is the extrapolated result independent of the basis parameters (or the "full-space" result within the set of symplectic irreps). The truncation error at each order N of the series expansion is given by  $\mathcal{O}(q^N)$ ; the leading-order error  $x_{N+1} = X_{N+1} - X_N$  is thus  $\mathcal{O}(qx_N)$ , which is consistent with effective-field-theory expansions for a sufficiently small expansion parameter (see, e.g., [52]). For results that largely depend on  $\hbar\Omega$ , extrapolated values for each  $\hbar\Omega$  significantly deviate; however, for  $\hbar\Omega$  values around the optimum one, deviations in  $X_{\infty}$  are drastically reduced, leading to relatively small uncertainties in the quoted extrapolated values.

### 4.1 Symmetry in low-lying excited states and giant resonances

The near symmetry is not restricted to ground states, but extends to low-lying states. For example, some yrast states have almost identical  $\operatorname{Sp}(3,\mathbb{R})$  structure to that of the ground state (e.g., see Ref. [1] for  $3_1^+$  and  $2_1^+$  in  $^6\operatorname{Li}$ , and for  $2_1^+$  and  $4_1^+$  in  $^{20}\operatorname{Ne}$ ; see also Fig. 6 for  $^{12}\operatorname{C}$ ). Practically the same symplectic content observed is a rigorous signature of rotations of a shape and can be used to identify members of a rotational band and enhanced B(E2) strengths.

Furthermore, the lowest  $1^-$  state in  $^{20}$ Ne is found to be largely dominated by the prolate (90)S = 0 shape, with some contribution from (52)S = 0 [53]. The second  $0^+$  state in  $^{20}$ Ne is dominated by two equilibrium shapes (Fig. 3a). It is interesting to note that the most deformed equilibrium shape for protons in the valence shell is (40), and the same for neutrons, resulting in overall shapes of (80), (42), and (04), the first of which dominates the ground state (Fig. 2a), whereas the (42) and (04) shapes

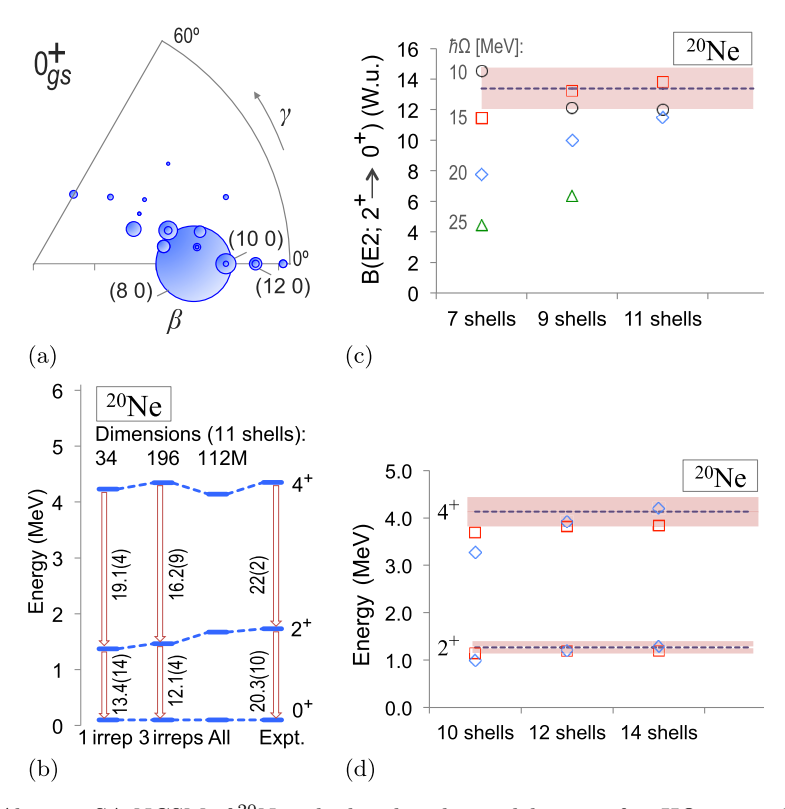


Fig. 2. Ab initio SA-NCSM of <sup>20</sup>Ne calculated in the model space of 11 HO major shells with the NNLO<sub>opt</sub> interaction [49] and  $\hbar\Omega=15$  MeV: (a) contribution of the symplectic Sp(3,  $\mathbb{R}$ ) irreps, given by the size of the circles, that make up the ground state of <sup>20</sup>Ne, calculated with an SU(3)-adapted basis in a selected model space of  $112\times10^6$  basis states (labeled as "All"); each irrep is specified by its equilibrium shape, labeled by the shape deformation  $\beta$  and triaxiality  $\gamma$ , with the largest contribution coming from the (80) shape; (b) observables calculated with the Sp(3,  $\mathbb{R}$ )-adapted basis using only the most dominant 1 or 3 symplectic irreps, as compared to experiment ("Expt."); dimensions of the largest model spaces used are also shown. Energies and reduced B(E2) transition strengths (in W.u.) are reported for extrapolations to infinitely many shells of converging results across variations in the number of shells and  $\hbar\Omega$ . (c, d) SA-NCSM calculations and the extrapolated central value (dashed line) and uncertainties (red shaded band) for the single most deformed Sp(3,  $\mathbb{R}$ ) irrep used in (b).

dominate the next 0<sup>+</sup> state for the NNLO<sub>opt</sub> interaction (Fig. 3a). Another interesting 0<sup>+</sup> state in <sup>20</sup>Ne is the lowest isobaric analog state (IAS), which corresponds to the lowest 0<sup>+</sup> state in the neighboring <sup>20</sup>Na and <sup>20</sup>F isotopes (Fig. 3b). This state manifests a dominance of a single prolate shape (61) that is slightly less deformed as compared to the (80) shape and is the main shape of the <sup>20</sup>Na and <sup>20</sup>F lowest 0<sup>+</sup> state where (80) is Pauli forbidden. It is important to emphasize that, besides the predominant irrep(s), there is a manageable number of symplectic irreps, each of which contributes at a level that is typically at least an order of magnitude smaller.

Nuclear saturation properties can be informed by nuclear breathing modes, or giant monopole resonances [55]. To study these, we calculate the response of the <sup>20</sup>Ne ground state to an isoscalar monopole probe  $M_0 = \frac{1}{2} \sum_i r_i^2$  (Fig. 4a). Since the  $M_0$  operator is a symplectic generator and does not mix symplectic irreps, the monopole response tracks the contribution of the (80) shape, the predominant shape of the <sup>20</sup>Ne

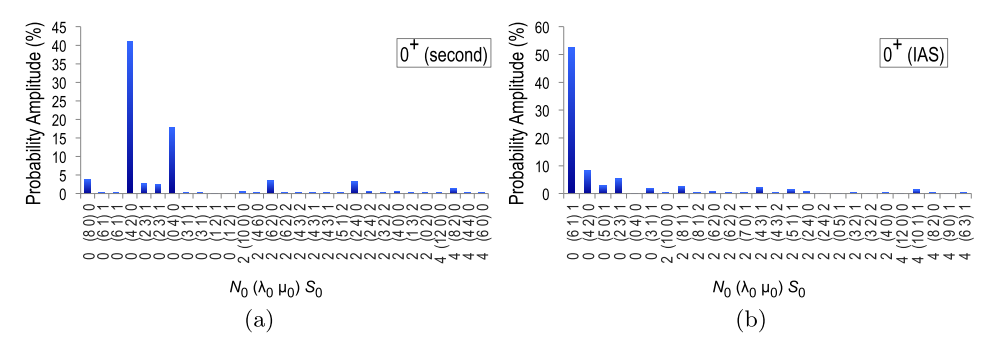


Fig. 3. Symplectic Sp(3,  $\mathbb{R}$ ) irreps that make up (a) the second  $0^+$  state and (b) the lowest  $0^+$  isobaric analog state (IAS) in <sup>20</sup>Ne, labeled by the total HO excitations  $N_0$ , SU(3) labels  $(\lambda_0 \mu_0)$ , and total intrinsic spin  $S_0$  of the equilibrium shape. Results are reported for *ab initio* SA-NCSM calculations with the NNLO<sub>opt</sub> interaction, for an SU(3)-adapted basis in a selected model space of 11 HO major shells and  $\hbar\Omega = 15 \,\text{MeV}$ .

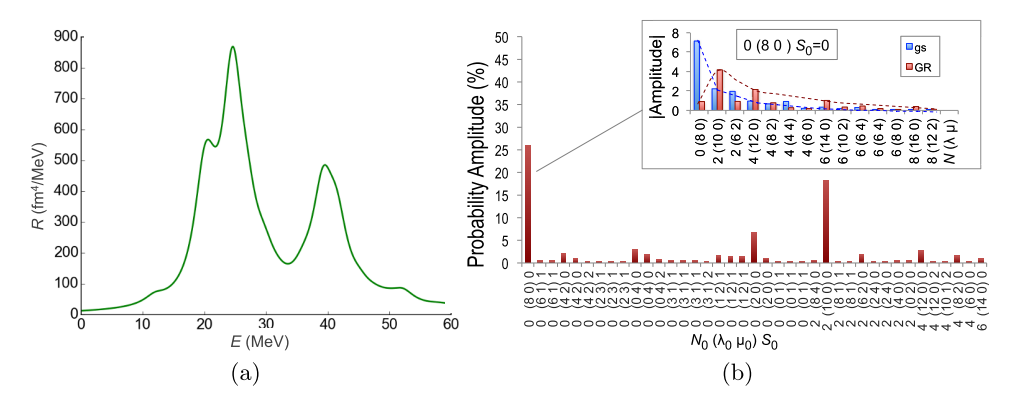


Fig. 4. (a) Monopole response function for the  $^{20}$ Ne ground state vs. excitation energy, for a width of  $\Gamma=2\,\mathrm{MeV}$  of the Lorentzian kernel [54]. (b) Symplectic Sp(3,  $\mathbb{R}$ ) irreps that make up the  $0^+$  excited state ("GR") that contributes the most to the giant resonance of  $^{20}$ Ne, labeled by the total HO excitations  $N_0$ , SU(3) labels ( $\lambda_0\,\mu_0$ ), and total intrinsic "GR" state along SU(3) configurations, labeled by the total HO excitations N and SU(3) labels ( $\lambda\mu$ ), as compared to the distribution of the same shape in the ground state ("gs"). Results are reported for *ab initio* SA-NCSM calculations that use the NNLO<sub>opt</sub> interaction for  $\hbar\Omega=15\,\mathrm{MeV}$ , and with an SU(3)-adapted basis in a selected model space of (a) 13 and (b) 11 HO major shells.

ground state, to all excited  $0^+$  states. It is not surprising then that the distribution and the peak of the response function are consistent with the results of reference [1], where the set of excited  $0^+$  states with nonnegligible contribution of the 1p-1h vibrations of the ground-state shape (80) has been suggested to describe a fragmented giant monopole resonance with a centroid around 29 MeV and a typical wavefunction spread out to higher deformation due to vibrations [56], as compared to the ground state (Fig. 4b, inset). Indeed, by examining the state that is related to the peak in the response function, we find that two equilibrium shapes dominate (Fig. 4b):  $N_0 = 0(80)S_0 = 0$  and  $N_0 = 2(100)S_0 = 0$ . The (80) also dominates the ground state, where it peaks at N = 0, while in the giant resonance state this shape peaks at the N = 2(100)S = 0 vibration (Fig. 4b, inset). Note that  $N_0 = 2(100)S_0 = 0$  is an equilibrium shape and N = 2(100)S = 0 is a dynamical shape, a vibration of

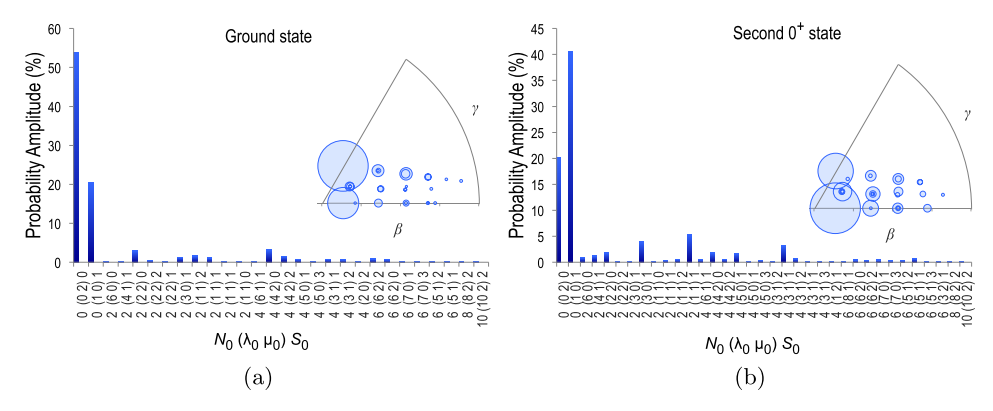


Fig. 5. Symplectic  $\operatorname{Sp}(3,\mathbb{R})$  irreps that make up (a) the  $0^+$  ground state and (b) the second  $0^+$  state of  ${}^8\mathrm{He}$ , labeled by the total HO excitations  $N_0$ ,  $\operatorname{SU}(3)$  labels  $(\lambda_0 \, \mu_0)$ , and total intrinsic spin  $S_0$  of the equilibrium shape, together with the corresponding  $\beta$ - $\gamma$  plot. Results are reported for *ab initio* SA-NCSM calculations with the NNLO<sub>opt</sub> interaction, for an  $\operatorname{SU}(3)$ -adapted basis in a complete model space of 14 HO major shells and  $\hbar\Omega = 20 \,\mathrm{MeV}$ .

the  $N_0 = 0(80)S_0 = 0$  equilibrium shape, but remarkably both have the same SU(3) quantum numbers.

Similarly, the lowest two  $0^+$  states in  $^8$ He, which has been suggested to be a halo nucleus, are made of a predominant shape that contributes at the 40–55% level and a secondary in importance shape with about 20% contribution (Fig. 5). It is interesting to note that both shapes are "opposite" in their deformation, (10) is prolate and the other one (02) is oblate (we note that another common convention associates a positive  $\beta$  value with a prolate shape, whereas a negative  $\beta$  indicates an oblate shape). While, in general,  $^8$ He is considered to be spherical, the present outcome points to an interplay of two shapes in the ground state, which on average may appear to have a zero deformation, but with a B(E2) strength from its  $2^+$  rotational state that constructively adds the nonzero contributions of both shapes.

### 4.2 Sensitivity to the NN interaction

The predominance of a few shapes is neither sensitive to the type of the realistic interaction used, nor to the parameters of the basis,  $\hbar\Omega$  and  $N_{\rm max}$  [1]. Details such as contribution percentages slightly vary, but dominant features retain. Furthermore, even when the NN interaction is trimmed down by removing many SU(3)-symmetric components that contribute less than a percent to the entire interaction, the results practically coincide with the corresponding ab initio calculations that use the full interaction [57]. As an illustrative example, we show that the SU(3) content for both the ground state and the lowest 2<sup>+</sup> state in <sup>12</sup>C remains practically the same when the full N3LO-EM [34] is used or its selected counterpart (Fig. 6). The corresponding matter rms radius deviates only by 1% when the selected interaction is used (Fig. 6a, inset), and such deviations typically decrease with larger model spaces (we note that in these calculations we neglect the three-nucleon forces that will reduce the deviation from the experimental value). This study offers another remarkable outcome, namely, chiral potentials such as N3LO-EM, when expressed as a sum of SU(3)-symmetric components, exhibit a clear dominance of its (00) component, which preserves deformation. In addition, we find that many of these components are negligible, which in turn makes the selection feasible.

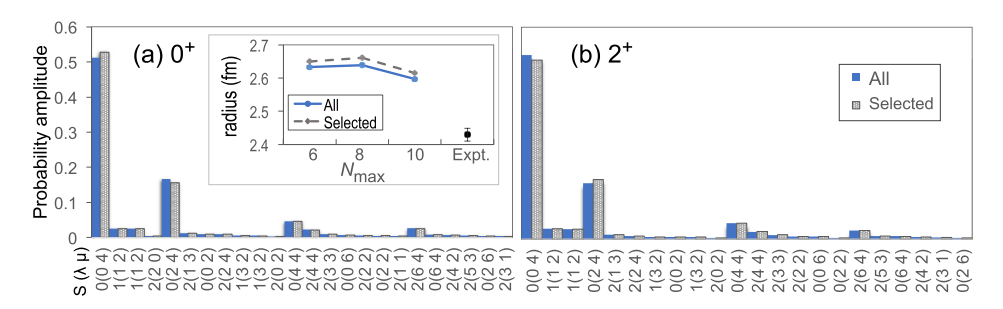


Fig. 6. SU(3) irreps that make up (a) the ground state and (b) the first  $2^+$  state of  $^{12}$ C, labeled by the total intrinsic spin S and SU(3) labels ( $\lambda \mu$ ). Results are reported for ab initio SA-NCSM calculations with the full N3LO-EM interaction [34] (solid blue) and its selected counterpart (dashed gray), for an SU(3)-adapted basis in a complete model space of 8 HO major shells and  $\hbar\Omega=15\,\mathrm{MeV}$ . Insets: matter rms radius of the  $^{12}$ C ground state as a function of the model space.

**Table 1.** Average energy per pair  $W_c$  (along the diagonal) and correlations  $\zeta$  of selected phase-equivalent NN interactions (including the Coulomb interaction between protons), given as  $(W_c^0, W_c^1)$  and  $(\zeta^0, \zeta^1)$  for (T=0, T=1) pairs, respectively. The NN part of two chiral potentials NNLO<sub>opt</sub>[49] and NNLO<sub>sat</sub> [65] is considered, along with a comparison to the JISP16 [45] based on the *J*-matrix inverse scattering method, for the two-nucleon system (A=2) and for a 12-particle system such as  $^{12}$ C (A=12, T=0). All interactions are reported for HO parameter  $1/b \sim 0.6 \, \mathrm{fm}^{-1}$ .

	$NNLO_{opt}$	$NNLO_{sat}$	JISP16	$NNLO_{opt}$	$NNLO_{sat}$
		A = 2		A = 12, T = 0	
$\overline{\mathrm{NNLO}_{\mathrm{opt}}}$	(-1.56, -0.19)				
$NNLO_{sat}$	(0.99, 0.86)	(-1.33, -0.54)		(0.92, 0.92)	
JISP16	(0.88, 0.84)	(0.88, 0.87)	(-1.31, -0.51)	(0.84, 0.84)	(0.88, 0.88)

Finally, the symplectic symmetry has been shown to ubiquitously arise from first principles regardless of the NN interaction and the type of nucleus. It is then interesting to address the question whether all NN interactions used in such calculations possess close similarity to each other, or if they deviate in certain features that appear to be inconsequential to the emergence of the symmetry. To study this, we consider average energies per pairs (centroids) and correlations [58] between various realistic interactions within the framework of spectral distribution theory [59–64] (Tab. 1). The outcomes show that the average energy for an isoscalar (isovector) pair is the largest (smallest) for NNLO<sub>opt</sub>, as compared to other interactions, whereas all of the interactions correlate strongly both at the level of the interaction itself and as propagated in, e.g.,  $^{12}$ C, with almost perfect correlation for the T=0 part of the NNLO<sub>sat</sub> and NNLO<sub>opt</sub>. In general, two interactions with the same eigenvectors have a correlation coefficient of  $\zeta = 1$ . Hence, the correlation outcome corroborates the above-mentioned results, that is, the same orderly pattern is observed in the eigenvectors for all these interactions, while the emergence of the symmetry appears not to be sensitive to the differences in the average energy.

In short, our findings show that nuclei below the calcium region, in their ground state as well as low-energy excitations, display relatively simple emergent physics that is collective in nature and tracks with an approximate symplectic symmetry heretofore gone unrecognized as emergent from the strong nuclear force. It is important to note that no new dominant shapes appear as we increase the model space, retaining the predominance of the single irrep, as shown in reference [1]. This has an important

implication: complete SA-NCSM calculations are performed in smaller model-space sizes to identify the nonnegligible symplectic irreps, while the model space is then augmented by extending these irreps to high (otherwise inaccessible) HO major shells. Accessing these shells is vital to account for collective and spatially enhanced modes. As these modes play an important role in nuclear structure and reactions modeling, the present outcome is key to achieving *ab initio* predictions, e.g., for short-lived isotopes with deformed or cluster structure along various nucleosynthesis pathways, especially where experimental measurements are incomplete or not available.

We acknowledge helpful discussions with D.J. Rowe, J.L. Wood, G. Rosensteel, J.P. Vary, P. Maris, C.W. Johnson, and D. Langr. This work was supported by the U.S. National Science Foundation (OIA-1738287, ACI -1713690, PHY-1913728), the Czech Science Foundation (16-16772S), and SURA, and in part by U.S. DOE (DE-FG02-93ER40756). This work benefitted from computing resources provided by Blue Waters, LSU (www.hpc.lsu.edu), the National Energy Research Scientific Computing Center NERSC (a DOE Office of Science User Facility supported under Contract No. DE-AC02-05CH11231), and TACC's Frontera resource (www.tacc.utexas.edu).

### Author contribution statement

All authors advanced the SA-NCSM framework, discussed the results and contributed to the final manuscript. In addition, K.D.L. implemented the computer codes for correlations and analyzed the results; T.D. implemented the suite of computer codes for the SA-NCSM and performed numerical simulations; G.H.S. implemented the computer codes for selected interactions, performed and analyzed numerical simulations; R.B.B. developed the theoretical formalism and implemented the computer codes for calculating response functions in the SA-NCSM, and performed the associated numerical simulations; and J.P.D. developed the theoretical formalism and computer package for SU(3) coupling/recoupling coefficients.

**Publisher's Note** The EPJ Publishers remain neutral with regard to jurisdictional claims in published maps and institutional affiliations.

### References

- T. Dytrych, K.D. Launey, J.P. Draayer, D.J. Rowe, J.L. Wood, G. Rosensteel, C. Bahri, D. Langr, R.B. Baker, Phys. Rev. Lett. 124, 042501 (2020)
- 2. D.J. Rowe, AIP Conf. Proc. **1541**, 104 (2013)
- T. Dytrych, K.D. Sviratcheva, C. Bahri, J.P. Draayer, J.P. Vary, Phys. Rev. Lett. 98, 162503 (2007)
- 4. K.D. Launey, T. Dytrych, J.P. Draayer, Prog. Part. Nucl. Phys. 89, 101 (2016) (review)
- J. Henderson et al., Phys. Lett. B 782, 468 (2018)
- P. Ruotsalainen, J. Henderson, G. Hackman, G.H. Sargsyan, K.D. Launey, A. Saxena, P.C. Srivastava, S.R. Stroberg, T. Grahn, J. Pakarinen, G.C. Ball, R. Julin, P.T. Greenlees, J. Smallcombe, C. Andreoiu, N. Bernier, M. Bowry, M. Buckner, R. Caballero-Folch, A. Chester, S. Cruz, L.J. Evitts, R. Frederick, A.B. Garnsworthy, M. Holl, A. Kurkjian, D. Kisliuk, K.G. Leach, E. McGee, J. Measures, D. Mücher, J. Park, F. Sarazin, J.K. Smith, D. Southall, K. Starosta, C.E. Svensson, K. Whitmore, M. Williams, C.Y. Wu, Phys. Rev. C 99, 051301 (2019)
- J. Williams, G.C. Ball, A. Chester, T. Domingo, A.B. Garnsworthy, G. Hackman, J. Henderson, R. Henderson, R. Krücken, A. Kumar, K.D. Launey, J. Measures, O. Paetkau, J. Park, G.H. Sargsyan, J. Smallcombe, P.C. Srivastava, K. Starosta, C.E. Svensson, K. Whitmore, M. Williams, Phys. Rev. C 100, 014322 (2019)

- 8. J.P. Elliott, Proc. Roy. Soc. A 245, 128 (1958)
- 9. M. Moshinsky, Rev. Mod. Phys. 34, 813 (1962)
- 10. J.P. Draayerm Y. Akiyama, J. Math. Phys. 14, 1904 (1973)
- 11. M. Moshinsky, J. Patera, R.T. Sharp, P. Winternitz, Ann. Phys. (N.Y.) 95, 139 (1975)
- 12. K.T. Hecht, W. Zahn, Nucl. Phys. A 318, 1 (1979)
- M.G. Mayer, J.H.D. Jensen, Elementary theory of nuclear shell structure (Wiley, New York, 1955)
- 14. J.P. Elliott, Proc. Roy. Soc. A 245, 562 (1958)
- 15. J.P. Elliott, M. Harvey, Proc. Roy. Soc. A **272**, 557 (1962)
- 16. V.K.B. Kota, SU(3) symmetry in atomic nuclei (Springer, Singapore, 2020)
- 17. K. Heyde, J.L. Wood, Rev. Mod. Phys. 83, 1467 (2011)
- 18. D.J. Rowe, Rep. Progr. Phys. 48, 1419 (1985)
- 19. G. Rosensteel, D.J. Rowe, Phys. Rev. Lett. 38, 10 (1977)
- 20. D.J. Rowe, G. Thiamova, J.L. Wood, Phys. Rev. Lett. 97, 202501 (2006)
- A.C. Dreyfuss, K.D. Launey, T. Dytrych, J.P. Draayer, C. Bahri, Phys. Lett. B 727, 511 (2013)
- 22. J.P. Draayer, K.J. Weeks, G. Rosensteel, Nucl. Phys. A 413, 215 (1984)
- G.K. Tobin, M.C. Ferriss, K.D. Launey, T. Dytrych, J.P. Draayer, C. Bahri, Phys. Rev. C 89, 034312 (2014)
- O. Castaños, P.O. Hess, J.P. Draayer, P. Rochford, Nucl. Phys. A 524, 469 (1991)
- 25. M. Jarrio, J.L. Wood, D.J. Rowe, Nucl. Phys. A **528**, 409 (1991)
- 26. C. Bahri, D.J. Rowe, Nucl. Phys. A **662**, 125 (2000)
- M. Freer, H. Horiuchi, Y. Kanada-En'yo, D. Lee, U. Meißner, Rev. Mod. Phys. 90, 035004 (2018)
- 28. K.D. Launey (ed.), Emergent phenomena in atomic nuclei from large-scale modeling (World Scientific Publishing Co., 2017)
- E. Caurier, G. Martinez-Pinedo, F. Nowacki, A. Poves, A.P. Zuker, Rev. Mod. Phys. 77, 427 (2005)
- 30. P. Navrátil, J.P. Vary, B.R. Barrett, Phys. Rev. Lett. 84, 5728 (2000)
- 31. B.R. Barrett, P. Navrátil, J.P. Vary, Prog. Part. Nucl. Phys. 69, 131 (2013)
- 32. P.F. Bedaque, U. van Kolck, Annu. Rev. Nucl. Part. Sci. 52, 339 (2002)
- E. Epelbaum, A. Nogga, W. Glöckle, H. Kamada, U.-G. Mei
  ßner, H. Witala, Phys. Rev. C 66, 064001 (2002)
- 34. D.R. Entem, R. Machleidt, Phys. Rev. C 68, 041001 (2003)
- 35. E. Epelbaum, Prog. Part. Nucl. Phys. **57**, 654 (2006)
- T. Dytrych, K.D. Launey, J.P. Draayer, P. Maris, J.P. Vary, E. Saule, U. Catalyurek, M. Sosonkina, D. Langr, M.A. Caprio, Phys. Rev. Lett. 111, 252501 (2013)
- 37. J.P. Draayer, Y. Leschber, S.C. Park, R. Lopez, Comput. Phys. Commun. 56, 279 (1989)
- K.D. Launey, T. Dytrych, J.P. Draayer, G.-H. Sun, S.-H. Dong, Int. J. Mod. Phys. E 24, 1530005 (2015) (review)
- T. Oberhuber, T. Dytrych, K.D. Launey, D. Langr, J.P. Draayer, Discrete & continuous dynamical systems-S (2020), DOI:10.3934/dcdss.2020383
- T. Dytrych, P. Maris, K.D. Launey, J.P. Draayer, J.P. Vary, M. Caprio, D. Langr,
   U. Catalyurek, M. Sosonkina, Comput. Phys. Commun. 207, 202 (2016)
- 41. T. Dytrych, A.C. Hayes, K.D. Launey, J.P. Draayer, P. Maris, J.P. Vary, D. Langr, T. Oberhuber, Phys. Rev. C **91**, 024326 (2015)
- 42. K.D. Launey, A. Mercenne, G.H. Sargsyan, H. Shows, R.B. Baker, M.E. Miora, T. Dytrych, J.P. Draayer, Emergent clustering phenomena in the framework of the ab initio symmetry-adapted no-core shell model, in Proceedings of the 4th International Workshop on "State of the Art in Nuclear Cluster Physics" (SOTANCP4), May 2018, Galveston, Texas, AIP. Conf. Proc. 2038, 020004 (2018)
- 43. A. Bohr, B.R. Mottelson, in *Nuclear structure* (Benjamin, New York, 1969), Vol. 1
- 44. O. Castaños, J.P. Draayer, Y. Leschber, Z. Phys. A **329**, 33 (1988)
- 45. A.M. Shirokov, J.P. Vary, A.I. Mazur, T.A. Weber, Phys. Lett. B 644, 33 (2007)
- A.C. Dreyfuss, K.D. Launey, T. Dytrych, J.P. Draayer, R.B. Baker, C.M. Deibel, C. Bahri, Phys. Rev. C 95, 044312 (2017)

- 47. B.J. Verhaar, Nucl. Phys. **21**, 508 (1960)
- 48. K.T. Hecht, Nucl. Phys. A 170, 34 (1971)
- A. Ekström, G. Baardsen, C. Forssén, G. Hagen, M. Hjorth-Jensen, G.R. Jansen,
   R. Machleidt, W. Nazarewicz et al., Phys. Rev. Lett. 110, 192502 (2013)
- 50. D. Shanks, J. Math. Phys. **34**, 1 (1955)
- C.M. Bender, S.A. Orszag, Advanced mathematical methods for scientists and engineers (McGraw-Hill, 1978)
- 52. J.A. Melendez, S. Wesolowski, R.J. Furnstahl, Phys. Rev. C 96, 024003 (2017)
- A.C. Dreyfuss, K.D. Launey, J.E. Escher, G.H. Sargsyan, R.B. Baker, T. Dytrych, J.P. Draayer, Phys. Rev. C (accepted), arXiv:2006.11208 (2020)
- R.B. Baker, K.D. Launey, S. Bacca, N. Nevo Dinur, T. Dytrych, Phys. Rev. C 102, 014320 (2020)
- 55. R. Baker, Electromagnetic Sum Rules and Response Functions from the Symmetry-Adapted No-Core Shell Model, Ph.D. Thesis, Louisiana State University, 2019
- 56. C. Bahri, J.P. Draayer, O. Castaños, G. Rosensteel, Phys. Lett. B 234, 430 (1990)
- G.H. Sargsyan, K.D. Launey, R.B. Baker, T. Dytrych, J.P. Draayer, Phys. Rev. C (submitted) (2020)
- 58. K.D. Launey, T. Dytrych, J.P. Draayer, Phys. Rev. C 84, 044003 (2012)
- 59. J.B. French, Phys. Lett. 23, 248 (1966)
- 60. J.B. French, K.F. Ratcliff, Phys. Rev. C 3, 94 (1971)
- 61. F.S. Chang, J.B. French, T.H. Thio, Ann. Phys. (N.Y.) 66, 137 (1971)
- 62. K.T. Hecht, J.P. Draayer, Nucl. Phys. A **223**, 285 (1974)
- 63. K.D. Sviratcheva, J.P. Draayer, J.P. Vary, Nucl. Phys. A **786**, 31 (2007)
- 64. V.K.B. Kota, R.U. Haq, Spectral distributions in nuclei and statistical spectroscopy (World Scientific Publishing Co., 2010)
- A. Ekström, G.R. Jansen, K.A. Wendt, G. Hagen, T. Papenbrock, B.D. Carlsson,
   C. Forssén, M. Hjorth-Jensen, P. Navrátil, W. Nazarewicz, Phys. Rev. C 91, 051301 (2015)